

A Reconfigurable Solar Photovoltaic Array Under Shadow Conditions

Dzung Nguyen, Brad Lehman

Email: nguyen.dun@neu.edu

ECE Department, Northeastern University, Boston, MA

Abstract - This paper proposes an adaptive reconfiguration scheme to reduce the effect of shadows on solar panels. A switching matrix connects a solar adaptive bank to a fixed part of a solar PV array, according to a model based control algorithm that increases the power output of the solar PV array. Control algorithms are implemented in real-time. An experimental reconfiguration PV system with the battery load is presented and is shown to verify the proposed reconfigurations.

Index Terms—Adaptive, Model-Based, Reconfiguration, Photovoltaic.

I. INTRODUCTION

MASS production and use of electricity generated from solar energy has become more common recently, perhaps because of the environmental threats arising from the production of electricity from fossil fuels and nuclear power. However, in many applications, such as solar power plants, building integrated photovoltaic, or solar tents, the solar photovoltaic arrays might be illuminated non-uniformly. The cause of non-uniform illumination may be the shadow of clouds, the trees, booms, neighbor's houses, or the shadow of one solar array on the other, etc. For example, Fig. 1 shows a portable, flexible solar array that is embedded into fabric. These new generation solar arrays can be folded and carried by campers and soldiers to remote locations. Often, they are left alone to charge batteries near trees, fences, and have been reported to even be wrapped around telephone poles or trees [1]. For these new applications, it has been especially important to optimize performance of the arrays in shadowed conditions.

Because of the nature of the electrical characteristics of solar cells, the maximum power losses are not proportional to the shadow, but magnify nonlinearly [2]. The shadow of solar PV array can cause many undesired effects:

- The real power generated from the solar PV array is less than designed, so that the loss of load probability increases [3].
- The local hot spot in the shaded part of the solar PV array

can damage the solar cells [1].

There are several approaches that have been proposed to reduce the effect of the shadow on the solar PV array output power:

1. Bypass diodes are connected across shadowed cells to pass the full amount of current while preventing damage to the solar cell [4], [5]. This method usually requires a great number of bypass diodes that are integrated in the solar arrays. The production of solar arrays with bypass diodes is more costly. Furthermore, the power losses of solar PV array are not prevented completely because of the power losses of the solar modules sorted by bypass diodes.

2. Alternatively, in large systems, each of the solar sub-modules can be connected to its own maximum power point (MPP) tracking DC-DC converter and can individually operate near its own MPP. Thus, the efficiency of the whole system is increased [6], [7], [8], but the method requires a large number of DC-DC converters (equal to the number of solar modules).

3. An emerging research field, and the focus of this paper, is to adaptively reconfigure solar array connections in real time in order to track maximum output power. Traditionally fixed solar PV arrays have hard wired interconnections between their solar cells. These connections are not changed after installation. However, it is possible to continuously rearrange solar cells in series and parallel connections [9] to facilitate the photovoltaic system to work more as a constant power source in even in different operating conditions (i.e. insolation, temperature, loads,...etc). Recent research studies in [10], [11] have started to develop methods to reconfigure solar cells to improve power output in shaded conditions. This research [10], [11] focus mostly on how to build the arrays, and does not propose real-time implementable control algorithm (the focus of this paper). Because of this, the methods proposed have unrealistic number of switches and sensors that must use complex control algorithms to determine when it turns the switch ON or OFF.

This paper develops new approaches for category 3 for adaptive reconfiguration of solar arrays that requires significantly fewer switches and voltages or current sensors than [10-11]. Further, for the first time published, simple control algorithm to determine how and when to adaptively reconfigure have been developed and experimentally tested.

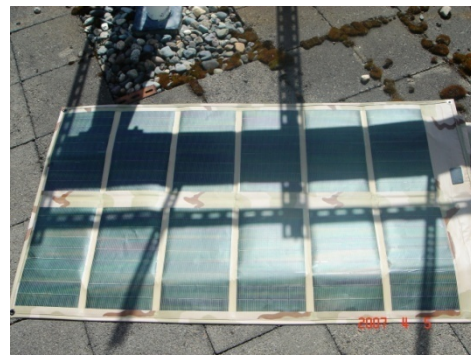


Fig. 1. Shadows on latest generation portable, flexible solar arrays

Specifically, this paper presents the following research contributions:

- (i) A new method for reconfiguration of solar PV arrays in real time under shadow conditions is presented. Solar cells from a (smaller) solar adaptive bank will be connected to the (larger) fixed part of the solar array. The maximum power point (MPP) of the whole array can be tracked by a single common maximum power point tracker (MPPT), instead of many MPPTs as shown in [5], [6], [7]. Since only a small percentage of the solar arrays are reconfigurable, fewer switches and simplified control algorithms are possible. In the uniform illumination conditions, all these adaptive solar cells will be equally connected to all rows of the fixed part of solar PV array. In non-uniform illumination conditions, the number of the adaptive solar cells connected to the shaded submodules depends on the shaded area of submodules. The reconfiguration is executed through the proposed switching matrix.
- (ii) Simple control decision algorithms are presented to determine when and how to open and close switches between the fixed part and adaptive bank of the solar PV array. One control algorithm relies on a trial-and-error bubble sort to increase solar PV array power. A second algorithm proposes to rely on model predictions. Both can be implemented in real-time by a micro-controllers or DSP and, to our knowledge, are the first time that such adaptive and implementable algorithm have been published.

- (iii) An experimental adaptively reconfigurable solar PV has been built and tested to verify proposed reconfigurations. It is shown that the approach proposed is able to increase output power of solar PV array in real-time under shaded conditions by 30% for a typical experiment.

II. DIFFERENT CONFIGURATIONS OF SOLAR PV ARRAYS AND THE MAXIMUM POWER LOSSES OF THE SHADOW

Fig. 2 shows the two common solar PV array configurations that utilize the combinations of the connections. In this figure, each $PV_{(i,j)}$ is an individual solar cell.

The solar cells are connected in series and parallel to create a solar array.

Simple series-parallel (SP) array:

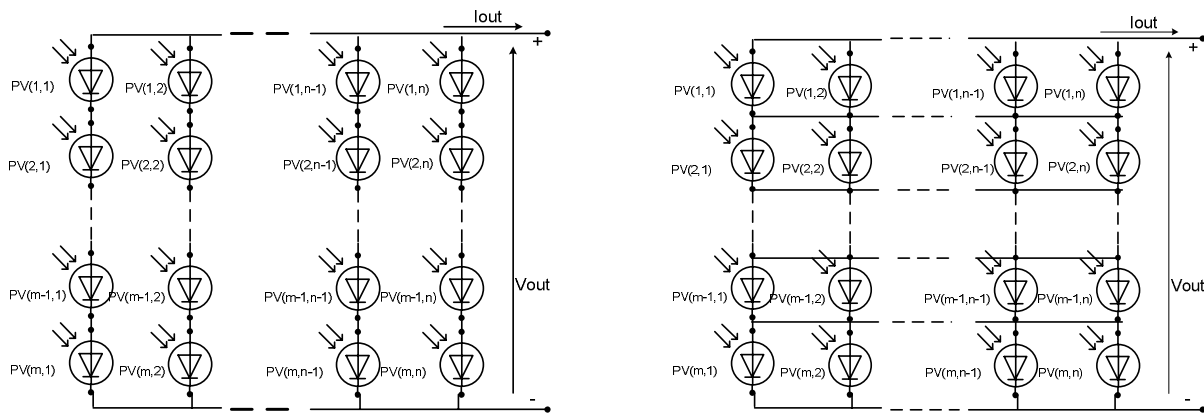
All solar cells, for example, $PV_{1,1}, PV_{2,1}, \dots, PV_{m-1,1}, PV_{m,1}$, are connected in series creating strings. Then all these strings are connected in parallel, as shown in Fig. 2(a).

Total-cross-tied (TCT) array:

All solar cells are connected in parallel, for example $PV_{1,1}, PV_{1,2}, \dots, PV_{1,n-1}, PV_{1,n}$ creating modules. Then these modules are connected in series, as shown in Fig. 2(b).

Fig. 3 shows a typical result of calculation of the power losses for SP and TCT for an array with 100 solar cells.

For SP connection, each solar cell in a different column completely shaded will cause 10% extra loss when shaded.



(a) Series-parallel interconnection (b) Total-cross-tied interconnection
Fig. 2. Solar PV array's common interconnections

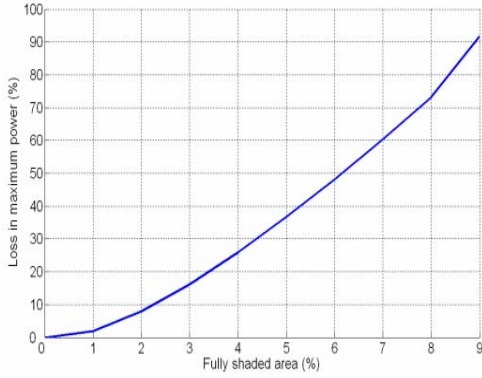


Fig. 3. The losses of maximum power depend on the shaded area. In SP one cell in each column is fully shaded. In TCT, one cell in each column, but in the same row is fully shaded.

If two solar cells in the same column are shaded, the power loss is still 10%.

For TCT connection, each solar cell in the same row completely shaded will cause 10% extra power loss. If two cells in different rows are shaded, the power loss is still 10%.

In the worst case of 10 fully shaded solar cells (10% of the total number of solar cells in the solar PV array), the maximum output power can be reduced more than 90%. The result is the same for both SP and TCT.

III. PROPOSED AN ADAPTIVE RECONFIGURATION METHOD

This section proposes a system architecture that permits adaptive reconfiguration of the connections between solar PV arrays. A switching matrix that connects a small reconfigurable bank of PV arrays with a larger non-reconfigurable bank of solar PV arrays is proposed. Because only the adaptive bank is being reconfigured, the number of switches and reconfiguration time seems tractable. We propose two different adaptive reconfiguration algorithms for the arrays, each of which will eventually produce the same increase in power under shadow conditions. The first method is simpler, and it relies on a serial bubble sort approach, which switches the adaptive PV arrays in one at a time. After each switching the power of the total system is analyzed and the next sort is implemented. In the second method, a model reference approach is proposed that is able to predict power levels in each of the rows of the fixed solar arrays and uses this prediction to simultaneously switch the connections of the adaptive bank.

In either case, the two different approaches eventually will produce the same increased power of the entire solar PV system, and both are implementable on a DSP in real time (see experimental results). However, the second approach is quicker, as we later experimentally demonstrate.

Fig. 4 shows the operation principle of the proposed method.

The fixed part: The fixed part is the main part of the solar array and has most number of solar cells, as shown in the Fig. 6. The fixed part contains of $(m \times n)$ solar cells (the solar cells $(1, 1), (1, 2), \dots, (m, n-1), (m, n)$).

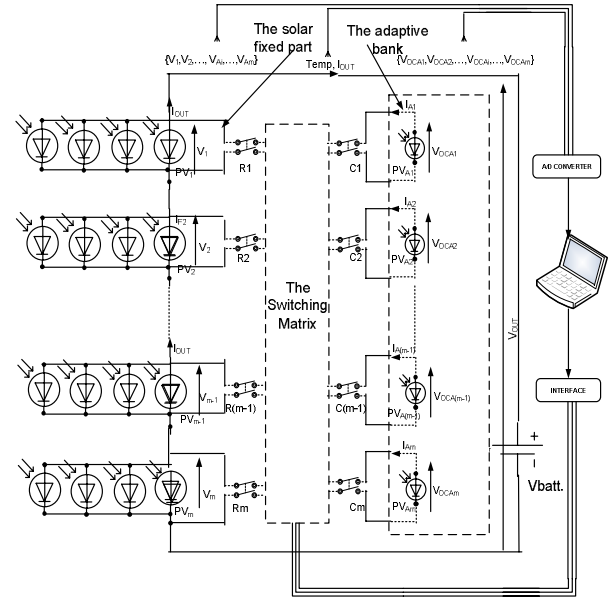


Fig. 4. Practical circuit of the proposed reconfiguration

All solar cells in the fixed part are connected by hard wire and have fixed configuration, with TCT, the total-cross-tied interconnection. We can consider that the fixed part of solar PV array has m PV “modules” connected in series.

The solar adaptive bank of solar cells: In this paper, the adaptive bank has m solar cells (the solar cells A_1, A_2, \dots, A_m) not connected together. These adaptive solar cells can be connected in parallel to any PV module, from PV_1 to PV_m , as seen in Fig. 4.

The switching matrix: The fixed part and solar adaptive bank are connected together through the switching matrix. The switching matrix, as shown in Fig. 5, contains switches $S(1, 1), S(1, 2), \dots, S(m-1, m-1), S(m, m)$ connect each solar cell in the adaptive bank to any row of solar cells in the fixed part of the PV array. When the switch $S(i, j)$ is ON the solar cell A_i from adaptive bank will be connected to row j of a fixed part. Thus, only one set of switches in a column can be ON at a time.

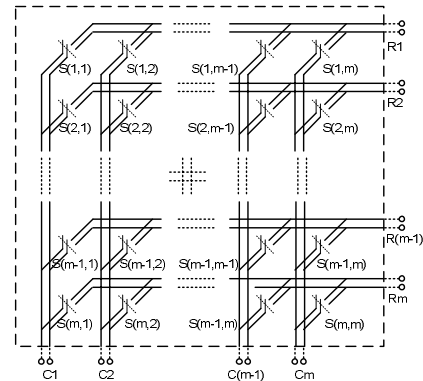


Fig. 5. The switching matrix

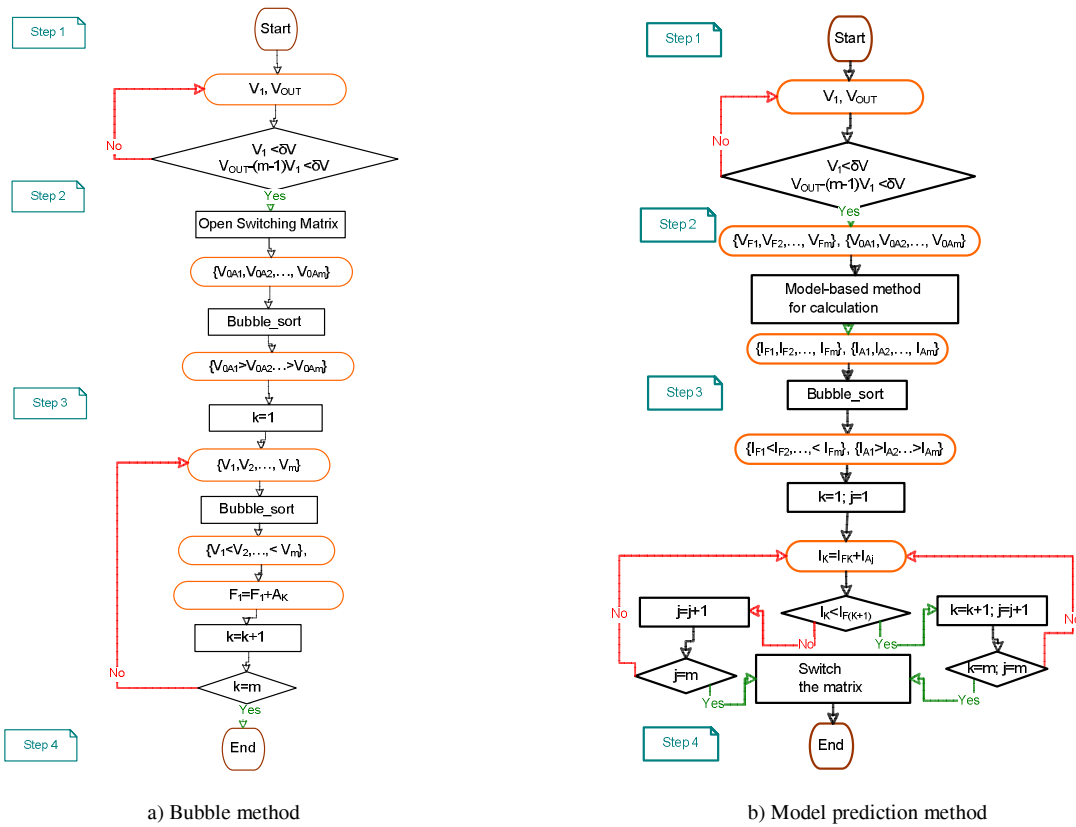


Fig. 6. The flowchart of two control algorithms

First method:

The flow chart of the first method is shown in Fig. 6(a). In general, the solar array is reconfigured by the following principle: if the voltage of one row is smaller than voltages of the other rows, it indicates that this row is the most shaded row. One solar cell from the adaptive bank will be switched in parallel to this row. The process will continue until all the solar cells of the solar adaptive bank are connected in parallel to the rows of the fixed part.

Step 1: The solar adaptive bank and fixed part of the solar array are connected together in the original configuration as in Fig. 4. The voltage V_1 and V_{OUT} are monitored, where V_1 is the voltage produced by row 1 of the solar array. In the uniform illumination, the output voltage: $V_{OUT} = m \times V_1$.

In the non-uniform illumination, two situations can occur:

The first case occurs when the first row is shaded and the other rows are non-shaded. In this case, the voltage of first row is reduced and it is less than the threshold voltage: $V_1 < \delta V$, the adaptive reconfiguration starts.

The second case occurs, when the first row is non-shaded, and at least one of the other rows is shaded, the output voltage of the solar array is not equal to $m \times V_1$, but much less than that: $V_{OUT} - (m - 1) \times V_1 < \delta V$. In this case also the adaptive reconfiguration starts.

Step 2: By opening all switches $S(1,1), S(2,2), \dots, S(m, m)$, all the solar cells in the solar adaptive bank are in the open circuits. Define and sort in decreasing order the open circuit voltages of all solar cells of the adaptive bank:

$$V_{0A1} > V_{0A2} > \dots > V_{0Am}$$

Step 3: Define the number of adaptive solar cells connected parallel to the shaded solar submodules in the fixed part.

Sorting: First, measure the voltages of all submodules of the solar fixed part. Next, the voltages of all submodules of the fixed part are sorted in

increasing order: $V_1 < V_2 < \dots < V_m$, the voltages of the fixed part. Thus, the rows of the fixed part and each adaptive solar cell have been renumbered according their sorting voltages.

Adding: Connect the solar cell with the maximum open circuit voltage of the solar adaptive bank in parallel to the most shaded sub-module of the fixed part, which has the smallest voltage. For example, if we switch solar cell A1 in parallel with the sub-module in row 1, then after the first switching, the solar adaptive bank becomes:

$$V_{0A2} > V_{0A3} > \dots > V_{0Am}$$

The fixed part might become:

$$V_2 < V_1 < \dots < V_m$$

Then the second switching occurs and the solar cell A2 is connected in parallel with the sub-module in the row 2. We continue the reconfiguration process until all the solar cells of the solar adaptive bank are connected parallel to the rows of the fixed part.

Step 4: When the shadow changes direction or shape, the voltage of the first row and the output voltage are continuously being measured and compared, and give the command to repeat the reconfiguration process, if the difference between them is above the fixed range, the control circuit repeats the procedure in Steps 2-3.

Second method:

The flow chart of the second method is shown in Fig. 6(b). The control algorithm to determine how to connect and reconfigure the solar cells is based on a model-based control method and contains the following steps:

Step 1: It is the same as Step1 in the first method

Step 2: Define the photo generated currents of all solar cells of the solar adaptive bank and of all submodules of the fixed part.

We can use model-based method to calculate the photo generated currents in Step 3. The benefits of this approach over the previous method is it defines photo generated currents of all solar cells of the solar adaptive bank and of all submodules of the fixed part, so all switches can be controlled synchronously at the same time.

The photo generated currents of the solar adaptive bank: By the opening all switches S(1,1), S(2,2), ..., S(m,m), all the solar cells in the solar adaptive bank are in the open circuits. By measuring the open circuit voltages of solar cells {V_{OCA1}, V_{OCA2}, ..., V_{OCAm}}, the photo generated currents I_{PHAj} are estimated by the following equation:

$$I_{Aj} = \frac{V_{OCAj}}{R_{SH}} + I_S * \left(\exp\left(\frac{qV_{OCAj}}{akT}\right) - 1 \right) \quad (1)$$

Here, R_{SH} - shunt resistance of solar cell, submodule, I_S - saturation current of the diode,

The photo generated currents of the fixed part: All submodules of the fixed part are still working with load. Their photo generated currents are calculated by the equation:

$$I_{Fj} = I_{OUT} + nI_S \left[\exp\left(\frac{q}{akT}(V_j + I_{OUT}R_{SM})\right) - 1 \right] + \left(\frac{V_j + I_{OUT}R_{SM}}{R_{SHM}} \right) \quad (2)$$

where, V_j={V₁, V₂, ..., V_m} - measured voltages of submodules, I_{OUT} - the output current of solar array, R_{SM} - series resistance of solar cell, submodule, R_{SHM} - shunt resistance of solar cell, submodule, I_S - saturation current of the diode, n - number of solar cells in submodule. These parameters of solar cell or solar submodule are received from manufacturers or extracted based on experiment by V-I curve fitting [16]. By updating temperature and voltage parameters in the model (in real-time) it is possible to estimate photo

generated currents I_{PHAj} and I_{PHFj} of each solar cell or submodule by using [12], [13] and their dynamics multi-physics models [17].

Step 3: Define the number of adaptive solar cells connected parallel to the shaded solar submodules in the fixed part

Sorting: First, the photo generated currents of all solar cells of the solar adaptive bank in the decreasing order:

$$I_{A1} > I_{A2} > \dots > I_{Am}, \text{ the current of the adaptive bank}$$

Next, the photo generated currents of all submodules of the fixed part are sorted in increasing order:

$$I_{F1} < I_{F2} < \dots < I_{Fm}, \text{ the currents of the fixed part.}$$

Thus, the rows of the fixed part and each adaptive solar cell have been renumbered according their sorting *predicted* photo generated current.

Adding: Connect the solar cell with the maximum predicted photo generated current of the solar adaptive bank in parallel to the most shaded sub-module of the fixed part. For example, if we switch solar cell A1 in parallel with the sub-module in row 1, then after the first switching, the solar adaptive bank becomes: I_{A2} > I_{A3} > ... > I_{Am}

The fixed part might become:

$$I_{F2} < I_{F1} + I_{A1} < \dots < I_{Fm}$$

Then the second switching occurs and the solar cell A2 is connected in parallel with the sub-module in the row 2. We continue the reconfiguration process until all the solar cells of the solar adaptive bank are connected parallel to the rows of the fixed part.

Step 4: When the shadow changes direction or shape, the voltage of the first row and the output voltage are continuously being measured and compared, and give the command to repeat the reconfiguration process, if the difference between them is above the fixed range, the control circuit repeats the procedure in Steps 2-3.

One example of the reconfiguration method is shown in Fig. 7. The solar PV array from 10x10 solar cells in the fixed part, 10 solar cells in the adaptive part has the interconnection in Fig. 7(a) - in the uniform illumination, in Fig. 7(b)- in the non uniform illumination.

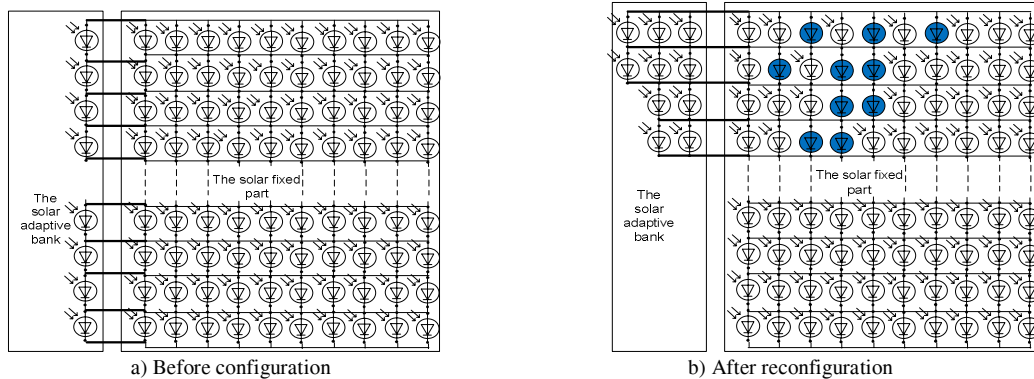


Fig. 7. Solar array's reconfiguration under non uniform illumination



Fig. 8. Solar PV array indoor test platform

Fig. 7 shows that by using the proposed adaptive reconfiguration method, when the number of shaded solar cells is less than the number of solar cells in one row, the maximum power loss is at most equals the power of the one row. If no adaptive bank and TCT connection, the shade would have up to 30% reduction in maximum output power (3 rows). With the adaptive bank, there is only 10% reduction in power.

IV. EXPERIMENT RESULT

Fig. 8 shows the solar PV array test platform. The experiment includes the following: The fixed solar array is from 12 solar cells, three rows and four columns (TCT connection). The solar adaptive bank combine from 3 solar cells (one string) connected to the fixed part (three strings), The 8 x 4 switching matrix, controlled by Agilent Data Acquisition/Switch Unit 34970A, is connected between the fixed part and the solar adaptive bank.

The voltages of solar cells in the solar adaptive bank and solar submodules in the fixed part are continuously measured and sent to PC running real-time MATLAB software. The sorting algorithm previously described is implemented by the PC in real-time.

First method: Fig. 9(a) shows the output voltage of the solar cells when 4 solar cells are partially shaded for first method. From time equal 0 to T_1 , the output voltage is under uniform illumination. From T_1 , solar PV array is shaded. The interval T_1 - T_2 is time for measurement and control. After T_3 , output voltage of solar array has been optimized and the reconfiguration has been completed. The changing output voltage from T_3 to T_4 is due to clouds moving across the array in this outdoor experiment (but the array has properly reconfigured to produce increased power). From T_4 - T_6 , the solar PV array is shaded by another shadow. The reconfiguration process is repeated as explained interval T_1 - T_3 .

The reconfiguration takes about 18 seconds. After the reconfiguration, the output voltage increases indicating increasing the power to the resistive load. In practice, the shadow of the object to the BIPV is slowly changed so that this reconfiguration control algorithm is fully applicable. In this experiment, the load resistor is 10 Ω . Thus, in the first shadow case, there is a 30% increase in output power after the reconfiguration.

Second method: Fig. 9(b) shows the output voltage of the solar cells when 4 solar cells are partially shaded for second method. From 0 to T_1 , the output voltage is under uniform illumination. From T_1 , solar PV array is shaded. The interval T_1 - T_2 is time for measurement and control. After T_2 , output voltage increases of solar array after reconfiguration. Notice that the voltage across the load is increased from T_2 , by 20% indicating a 46% increases in power due to reconfiguration. The output voltage of solar array initially drops during real time reconfiguration (between T_1 and T_2). This is because the solar adaptive bank is disconnected from the load for short time to measure and sort. During the transition, though, the fixed part is still supplying power for the load.

From T_3 - T_4 , the solar PV array is shaded by another shadow. The reconfiguration process is repeated as explained interval T_1 - T_2 .

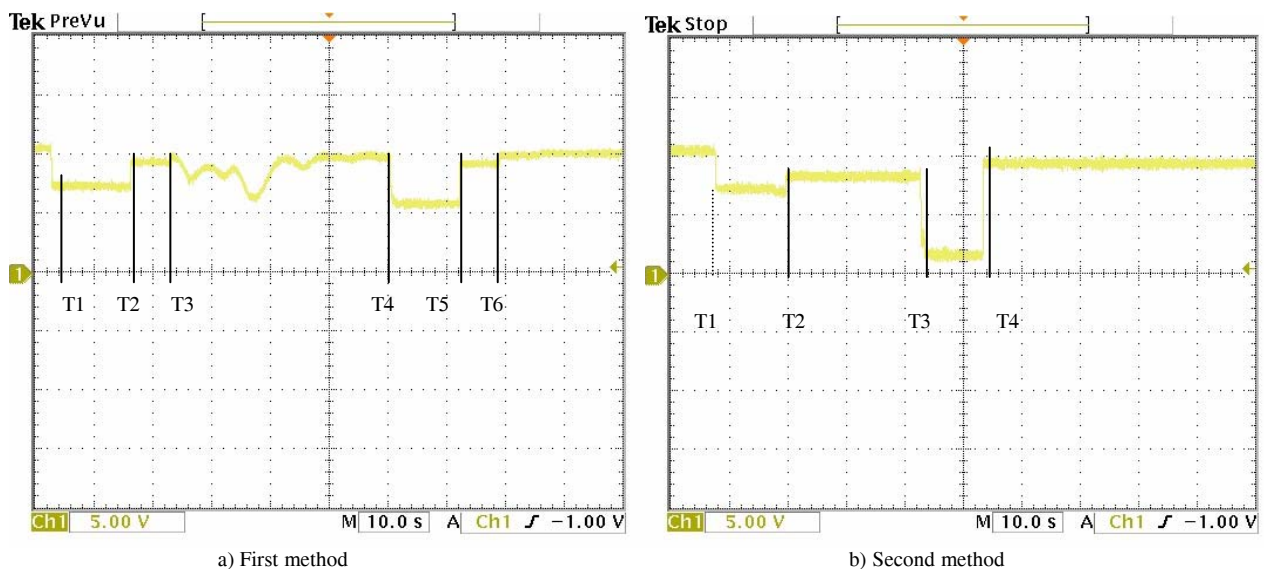


Fig. 9. Output voltage of solar PV array before and after reconfiguration:

Comparison between first and second methods

The second reconfiguration method takes about 8 seconds. This method is faster because all switches can be controlled synchronously at the same time, when the first method switches one at a time instead of all at once.

V. CONCLUSIONS

A new approach for adaptive reconfiguration of solar PV arrays under shadow conditions is described. A matrix of switches is used to connect a “fixed” total- cross- tied array with an adaptive array that can be reconfigured. Simple control algorithms are presented that determine how to control the switches to optimize output power. An experimental adaptively reconfigurable solar PV array has been built and tested to verify the proposed configurations.

The switching matrix is working in at relatively low switching frequency, so the electromechanical relays can be used to increase the current going through panels. The number of voltage sensors can be increased if it is desired to reduce the calculation time. The simple sorting algorithm is applied to reduce the calculation time.

The proposed reconfiguration method helps avoid the local maximum power points of solar PV arrays, thus the central maximum power point tracker can be used to track the maximum output power of the whole solar PV array.

ACKNOWLEDGEMENT

This article was funded in part by a grant from the Vietnam Education Foundation (VEF). The opinions, findings, and conclusions stated herein are those of the authors and do not necessarily reflect those of VEF.

NOMENCLATURE

I_{Aj}	photo generated current of solar in the adaptive bank
V_{OCAj}	open-voltage of solar cell A_j
R_{SH}	shunt resistance of solar cell, submodule
I_S	saturation current of the diode,
a	ideality factor of bypass diode
k	Boltzman’s constant.
T	cell operating temperature
q	electron charge
I_{Fj}	photo generated current of submodules in the fixed part
V_j	voltages of submodules,
I_{OUT}	the output current of solar array
R_{SM}	series resistance of solar cell, submodule
R_{SHM}	shunt resistance of solar cell, module
n	number of solar cells in submodule

REFERENCES

- [1] F. Jeffrey, *Power Film Inc.*, Private communication
- [2] S. H. Raushenbach, “Electrical output of shadowed solar arrays,” *IEEE Transaction Electronic Devices*, vol. 18, p. 483, Aug. 1971
- [3] Ward T. Jewell, Timothy D. Unruh “Limits on Cloud-Induced Fluctuation in Photovoltaic Generation”, *IEEE Transactions on Energy Conversion*, Vol. 5, No. 1, March 1990.
- [4] M. S. Swaleh, M. A. Green, “Effect of shunt resistance and bypass diode on the shadow tolerance of solar cell modules,” *Solar Cells*, Vol. 5, No. 2, 1982.

- [5] N. F. Shephard, R. S. Sugimura, “The integration of bypass diode with terrestrial photovoltaic modules and arrays,” *Proceedings 17th IEEE Photovoltaic Specialist Conference*, 1984.
- [6] Hisao Watanabe, Toshihisa Shimizu, Gunji Kimura, “A Novel Utility Interactive Photovoltaic Inverter with Generation Control Circuit,” *IEEE Industry Electronics Society*, 1998.
- [7] Toshihisa Shimizu, Masaki Hirakata, Tomoya Kamezawa, and Hisao Watanabe, “Generation Control Circuit for Photovoltaic Modules,” *IEEE Transaction On Power Electronics*, Vol.16, No.3 May 2001.
- [8] Roman E., Ibanez P., Elorduizaparietxe S., Alonso R., Goitia D., Martinez D. Alegria, “Intelligent PV module for Grid-Connected PV system,” *IEEE Industrial Electronics Conference*, 2-6 November 2004.
- [9] El-Shibini, M.A., Rakha, H.H.” Maximum power point tracking technique,” *Electro technical Conference Proceedings, MELECON '89, Mediterranean*, 11-13 April 1989.
- [10] Chin Chang “Solar Cell Array Having Lattice or Matrix Structure and Method Of Arranging Solar Cells and Panels,” *Patent No.: US 6,635,817 B2*, Oct. 21, 2003.
- [11] Raed A. Sherif, Karim S. Boutros, Moorpark United States Patent “Solar Module Array with Reconfigurable Tile,” *Patent No. US 6,350,944 B1*, Feb, 26, 2002.
- [12] V.Quaschnig and R. Hanitsch, “Numerical simulation of current-voltage characteristics of photovoltaic systems with shaded solar cells,” *Solar Energy*, Vol. 56, No. 6, 1996.
- [13] D.D. Nguyen, Brad Lehman “Modeling and Simulation Solar PV Arrays under Shadow Conditions”, *COMPEL 2006*, 16-19 July, 2006.
- [14] Narendra D. Kaushika and Nalin K. Gautam “Energy Yield Simulations of Interconnected Solar PV Arrays,” *IEEE Transaction on Energy Conversion*, vol. 18, No. 1, March 2003, pp. 127-134.
- [15] V.Quaschnig and R. Hanitsch, “Influence of shading on electrical parameters of solar cells,” *Photovoltaic Specialists Conference*, 13-17 May, 1996.
- [16] Wilhelm Durisch and Jean-Claude Mayor “Application of A Generalized Current Voltage Model for Module Solar Cells to Outdoor Measurement On a Siemen SM 110-Module,” *3rd World Conference on Photovoltaic Energy Conversion* May 11-18, 2003.
- [17] Shengyi Liu, Roger A. Dougal, “Dynamic Multiphysics Model for Solar Array,” *IEEE Transaction on Energy Conversion*, vol. 17, No. 2, June 2002.